Self-propelled Vicsek particles at low speed and low density

M. Leticia Rubio Puzzo,[1,2,3] Andrés De Virgiliis,[1,2,4] and Tomás S. Grigera[1,2,3]

[1]*Instituto de Física de Líquidos y Sistemas Biológicos (IFLYSIB), CONICET y Universidad Nacional de La Plata,*
Calle 59 no. 789, B1900BTE La Plata, Argentina
[2]*CCT CONICET La Plata, Consejo Nacional de Investigaciones Científicas y Técnicas, B1904CMC La Plata, Argentina*
[3]*Departamento de Física, Facultad de Ciencias Exactas, Universidad Nacional de La Plata, 1900 La Plata, Argentina*
[4]*Departamento de Ciencias Básicas, Facultad de Ingeniería, Universidad Nacional de La Plata, 1900 La Plata, Argentina*

We study through numerical simulation the Vicsek model for very low speeds and densities. We consider scalar noise in two and three dimensions and vector noise in three dimensions. We focus on the behavior of the critical noise with density and speed, trying to clarify seemingly contradictory earlier results. We find that, for scalar noise, the critical noise is a power law in both density and speed, but although we confirm the density exponent in two dimensions, we find a speed exponent different from earlier reports (we consider lower speeds than previous studies). On the other hand, for the vector noise case we find that the dependence of the critical noise cannot be separated as a product of power laws in speed and density. Finally, we study the dependence of the relaxation time with speed. At the critical point we find a power law, with the same exponent in two and three dimensions.

I. INTRODUCTION

The Vicsek model (VM) [1] was proposed more than 20 years ago as a minimal model of flocking and swarming [2]. Since then it has been widely studied [3] and has established itself as sort of yardstick for flocking models. Aside from its applications in understanding the microscopic mechanisms underlying swarming phenomena as observed in fish, birds, or mammals [4], it has attracted the attention of statistical physicists as a simple realization of a model of self-propelled particles, i.e., out-of-equilibrium models where the speed of particles is maintained by a nonconservative source of energy [5].

In the VM each particle moves with a fixed speed v_0, and at each step the velocity is rotated so as to align with the average velocity of its neighbors (with some noise η leading to nonperfect alignment). This aligning interaction leads to the development of order (flocking phase) at low noise and high number density (ρ), the order parameter φ being the system's average, or center-of-mass, velocity. This is superficially similar to the order arising in lattice spin models such as Ising or Heisenberg, but a crucial feature of the VM is the coupling between density and order parameter [6]: a density fluctuation that results in a local density higher that the critical one will result in a small cluster of ordered particles, but since ordered (i.e., velocity-aligned) particles travel together, these particles will tend to stay together, while "capturing" misaligned particles that by chance arrive in the neighborhood, thus enhancing density fluctuations.

This coupling of order parameter and density is largely responsible for the most salient features of the VM, namely, [7] (1) the existence of an order-disorder transition, controlled by density or noise, with the emergence of a phase with long-range order in the velocity, even in two dimensions, (2) the existence of propagating modes (density waves) in the ordered phase, and (3) a growth of the variance of the number of particles found in a given volume that is faster than linear in the number of particles (giant number fluctuations).

So in contrast to lattice spin models, the speed v_0 of the particles is more than simply a scale of measurement, because while the alignment interaction is independent of v_0, the displacement of the particles in space is not, so that changing the speed alters the coupling of density and order parameter, and a change of v_0 cannot be compensated by a rescaling of time. In fact the speed is a *thermodynamic* parameter, since the critical values η_c and ρ_c of noise and number density at which the order-disorder transition occurs depend on v_0. The aim of this article is to study the thermodynamic and dynamic effects of variations in v_0 in the low-density, low-speed regime.

When $v_0 = 0$ (but keeping nonetheless a direction vector so that the interaction can be defined), the VM reduces in three dimensions to the classical Heisenberg model on a (random) graph (XY model in two dimensions). For low enough density, most particles will be disconnected, and the system will remain disordered for all values of the noise. One thus expects $\eta_c \to 0$ for $v_0 \to 0$ at low densities, but the exact dependence of η_c with ρ and v_0, as well as the dynamical effects of the reduction in speed, have not been thoroughly studied up to now.

The findings of published studies can be summarized as giving a power-law dependence of the critical noise on both speed and density,

$$\eta_c \sim v_0^\sigma \rho^\kappa, \tag{1}$$

although not all works study both variables simultaneously. There are, however, differences in the reported values of the

exponents, as well as in the theoretical arguments supporting them. Czirók *et al.* [8,9] were the first to report a power-law dependence of η_c; they found numerically $\kappa = 0.25(5)$ in one dimension and $\kappa = 0.45(5)$ in two dimensions.

Some time later, Chaté *et al.* [10] studied the phase diagram in the (η, ρ, v_0) parameter space. They argued that in the diluted limit ($\rho \ll 1/r_c^d$ where r_c is the interaction radius) the critical value of the noise should behave as $\eta_c \sim v_0\rho^{1/d}$, i.e., $\kappa = 1/d$, $\sigma = 1$. The ρ dependence was confirmed numerically in two and three dimensions, but the linear v_0 dependence was tested only in two dimensions and at relatively high speeds. This is compatible with the findings of Refs. [8,9] for two dimensions but not with $\kappa = 0.25$ for one dimension However, the one-dimensional version of the model was defined in these references with some modifications that maybe responsible for the disagreement. Baglietto and Albano [11] argued from numerical simulation (in two dimensions) that η_c tends to a finite limit when $v_0 \rightarrow 0$; however, the analysis was done at $\rho = 0.25$, and $v_0 \geqslant 5 \times 10^{-3}$ (about two orders of magnitude above the speed values analyzed in the present study). More recently, Ginelli [3] revisited the issue and gave a modified argument (reviewed below in Sec. III A and the Appendix), arguing instead that $\eta_c \sim \sqrt{\rho}$, which agrees with Ref. [10] only in two dimensions. However, the three-dimensional (3D) case was not examined in this work.

In summary, though there seems to be agreement that $\eta_c \sim \sqrt{\rho}$ in two dimensions, the speed dependence, as well as the density dependence in different dimensions, deserves further consideration. It should also be mentioned that there are two variants of the VM in common use, which introduce the noise in different ways (scalar noise and vector noise, as explained below). The works quoted above use either one of the variants, and it is not clear whether the kind of noise has some influence on the differences found.

In the present work, we revisit the VM in two and three dimensions, paying special attention to the η_c dependence with speed and density, in the slow and diluted limit.

The paper is organized as follows: Sec. II reviews the definition of the VM and gives details of the simulations, results are presented in Sec. III, and Sec. IV states our conclusions.

II. MODEL AND SIMULATION DETAILS

The VM consists of N self-propelled particles endowed with a fixed speed v_0 and moving in d-dimensional space. At each time step, positions $\mathbf{r}_i(t)$ and velocities $\mathbf{v}_i(t)$ are updated according to

$$\mathbf{v_i}(t + \Delta t) = v_0 \mathcal{R}_\eta \left[\sum_{j \in S_i} \mathbf{v}_j(t) \right], \qquad (2)$$

$$\mathbf{r_i}(t + \Delta t) = \mathbf{r}_i(t) + \Delta t \mathbf{v}_i(t + \Delta t), \qquad (3)$$

where S_i is a sphere of radius r_c centered at $\mathbf{r}_i(t)$. The operator R_η normalizes its argument and rotates it randomly within a spherical cone centered at it and spanning a solid angle $\Omega_d \eta$, where Ω_d is the area of the unit sphere in d dimensions ($\Omega_2 = 2\pi$, $\Omega_3 = 4\pi$).

The order parameter, which measures the degree of flocking, is the normalized modulus of the average velocity [1,2],

$$\varphi \equiv \frac{1}{N v_0} \left| \sum_{i=1}^{N} \mathbf{v}_i \right|. \qquad (4)$$

Here $\varphi \in [0, 1]$, with $\varphi = O(1/\sqrt{N}) \sim 0$ in the disordered phase and $\varphi = O(1)$ in the the ordered phase. We choose $\Delta t = r_c = 1$, so that the control parameters are the noise amplitude η, the speed v_0, and the number density $\rho = N/V$, where $V = L^d$ is the volume of the (periodic) box.

The update rule for the positions, Eq. (3), is known as the *forward update* and was first used by Chaté *et al.* [10]. The original VM [1] used instead the so-called *backward update* rule, i.e., $\mathbf{r}_i(t + \Delta t) = \mathbf{r}_i(t) + \Delta t \mathbf{v}_i(t)$. It is generally agreed [3] that choosing either prescription results in essentially the same behavior for $t \rightarrow \infty$, although a small shift toward higher values of η_c has been reported for backward update [12]. We have only used forward update in this work.

Equation (2), a d-dimensional generalization of the original direction update rule, uses what is known as *scalar noise*. Scalar noise corresponds to a single source of noise in the alignment (e.g., the local average velocity is measured exactly, but the adjustment of the direction is subject to noise). An alternative way to introduce noise which we also consider below is to use random vectors. The first definition of this kind of *vector noise* is due to Czirók *et al.* [13]:

$$\mathbf{v_i}(t + \Delta t) = v_0 \mathcal{N} \left[\mathcal{N} \left(\sum_{j \in S_i} \mathbf{v}_j(t) \right) + \boldsymbol{\xi} \right], \qquad (5)$$

where $\mathcal{N}(\mathbf{v}) = \mathbf{v}/|\mathbf{v}|$ and $\boldsymbol{\xi}$ is a vector uniformly distributed on a sphere of radius η. Years later, Grégoire and Chaté [14] introduced an alternative definition of vector noise. Calling N_{ij} the number of particles in the neighborhood of S_i, they defined

$$\mathbf{v_i}(t + \Delta t) = v_0 \mathcal{N} \left[\sum_{j \in S_i} \mathbf{v}_j(t) + N_{ij} \boldsymbol{\xi} \right]. \qquad (6)$$

The idea of this rule is that there are multiple sources of noise, e.g., in recording the velocity of each neighbor. Most of the 3D simulations presented in this work have been performed with Eq. (5), but we have also considered the rule given by Eq. (6) in some particular cases. For rather low densities used in this work, the two definitions should not make much of a difference; this expectation is fulfilled in our comparisons and is supported by the behavior of η_c versus ρ shown in the inset of Fig. 8 below.

A qualitative idea of the behavior of the model can be gathered from the simulation snapshots in Fig. 1, where we show an example of ordered and disordered configurations in two and three dimensions

We studied the two-dimensional (2D) and 3D VM by standard Monte Carlo simulation, using a simulation box of size L^d with periodic boundary conditions. In two dimensions we used densities $\rho = 0.1$ and $\rho = 1.0$ with $500 \leqslant N \leqslant 10240$ particles, while in three dimensions, $N = 1000$ and densities in the range $\rho = 10^{-3}$ to $\rho = 1$. This corresponds to box
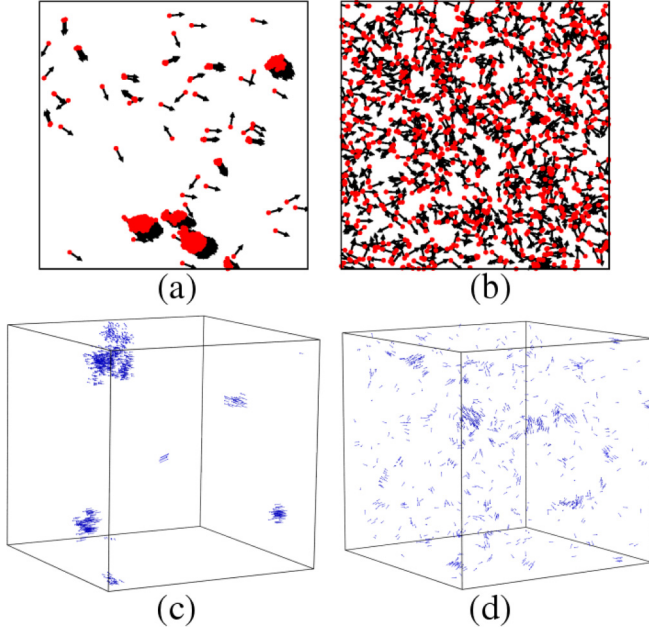
FIG. 1. Snapshots for $N = 10^3$ in two and three dimensions. 2D configurations for $\rho = 1.0$, $v_0 = 10^{-4}$, and (a) $\eta = 0.005 < \eta_c(\rho, v_0)$; (b) $\eta = 0.015 > \eta_c(\rho, v_0)$. The 3D case for $\rho = 0.01$, $v_0 = 10^{-2}$; and (c) $\eta = 10^{-4} < \eta_c(\rho, v_0)$; (d) $\eta = 10^{-2} > \eta_c(\rho, v_0)$.

sides $L = (N/\rho)^{1/d}$ in the range $L \simeq [22, 320]$. The range of speeds considered was from $v_0 = 10^{-1}$ to $v_0 = 10^{-5}$ in two dimensions, and $v_0 = 1$ to $v_0 = 10^{-2}$ in three dimensions. The system sizes we consider are smaller than those used in recent studies of the order transition or phase separation on the VM. Very large system sizes are important when considering, e.g., the nature of the transition [10], but here we are concerned with the location of the transition, and not with its nature, and we explore, rather than precise values of η_c, general trends: is the dependence power law? Can we estimate the exponents? We can accurately detect the transition as described in Sec. III A independently of its smoothing, and we do not see significant size effects in the quantities we study (see, e.g., Fig. 5 below).

Unless otherwise stated, simulations were started from a completely disordered initial condition, i.e., position and direction of motion [$\mathbf{r}_i(t = 0)$ and $\mathbf{v}_i(t = 0)$] chosen randomly. In some cases we used a completely ordered initial state, where all particles are assigned the same velocity and distributed in a sphere of radius $2r_c$.

All results shown correspond to observables measured at the stationary state, which we have checked up to second order (i.e., for one- and two-time quantities). We estimated the time needed to reach the stationary state in two different ways. First, we recorded the time t_{st} required for two systems with identical parameters, one starting from a completely disordered state [$\varphi(t = 0) \sim 0$] and another one starting from complete order ($\varphi(t > t_{st}) = 1$), to reach the same value φ [see Fig. 2(a)]. In addition, we estimated the correlation time from the (connected) time correlation function of the order parameter,

$$C(t) = \langle (\varphi(t_0) - \langle\varphi\rangle)(\varphi(t + t_0) - \langle\varphi\rangle)\rangle, \quad (7)$$
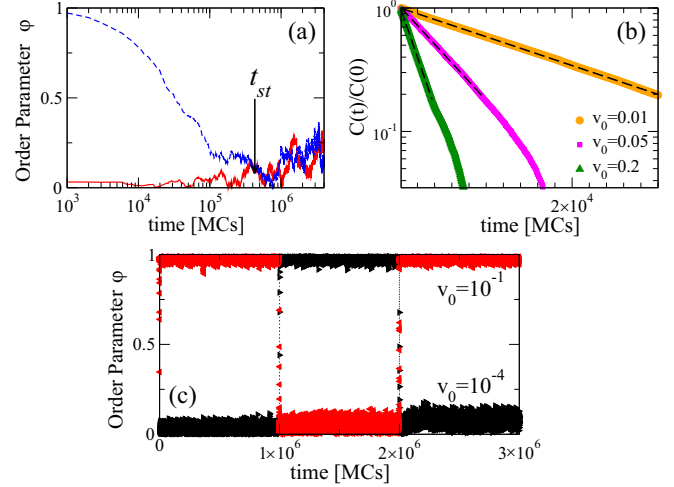

FIG. 2. (a) Two dimensions: Time evolution of the order parameter starting from disordered (full line) and ordered (dashed line) condition for $N = 10^3$, $\rho = 0.1$, and $v_0 = 10^{-4}$ at $\eta = \eta_c(v_0, \rho)$. (b) Three dimensions: Initial evolution of the time correlation function $C(t)/C(0)$ for $N = 1000$, $\rho = 0.01$, and different v_0, as indicated. Dashed line corresponds to the exponential decay fit [$C(t) \simeq e^{-t/\tau}$]. (c) Two dimensions: Time evolution of the order parameter φ, for $\eta = 0.01$, $N = 10^3$, and $\rho = 1.0$ when abruptly changing the speed v_0 from 10^{-1} to $v_0 = 10^{-4}$ and back (black-right triangles), and from 10^{-4} to $v_0 = 10^{-1}$ and back (red-left triangles).

where $\langle \ldots \rangle$ stands for an average over different simulation runs and time origins t_0. The correlation time τ was then estimated from an exponential fit of the initial decay of $C(t)$ [see Fig. 2(b)]. Figures 2(a) and 2(b) show typical curves used to obtain t_{st} and τ, respectively. Full results for t_{st} and τ are shown below (Sec. III B); essentially t_{st} is about four to five times τ. In our measurements we have therefore discarded all data for $t < t_{st}$ and used time series of at least 10τ (100τ in two dimensions). We have also checked that there are no aging effects in the time intervals studied, i.e., that $C(t)$ is independent of t_0.

As an additional precaution, for some values of ρ and v_0 we have performed the following check: after the order parameter had reached a stationary value in the ordered phase, we changed abruptly the speed to a value corresponding to the disordered phase, then back again to its original value. A similar check but starting from a disordered state was also done [see Fig. 2(c)]. The absence of hysteresis confirms that the simulation times are such that we are investigating a stationary state independent of the initial conditions.

III. RESULTS AND DISCUSSION

A. Speed and density dependence of the critical noise

To see why the critical noise depends on density, one can give a rough argument for very dilute systems, arguing that two particles emerge from an encounter agreeing on their orientations, but slowly move apart and their velocities start to drift. If the particle encounters another one before completely forgetting the common orientation of the previous collision, then order can propagate [3,10]. Thus one estimates the onset of order equating the *persistence length* (distance traveled

before losing the out-of-collision heading) and the *mean-free path* (distance traveled between collisions). One concludes that $\eta_c \sim \sqrt{\rho}$ [3], independent of dimension (the argument is reviewed in the Appendix). However, because it assumes instantaneous collisions (i.e., that the time between collisions is much larger than the time spent at relative distance less than the interaction radius r_c), the argument breaks down when $v_0 \to 0$ (see the Appendix). In two dimensions, $\eta_v \sim \sqrt{\rho}$ was also found more rigorously in a hydrodynamic treatment of the VM [15].

The dependence with v_0 is more difficult to understand, but its relevance on determining η_c is intuitive given the known importance of the coupling between density fluctuation (driven by particle displacements) and order parameter. When the speed is reduced, groups of aligned particles tend to stick together longer (enhancing order), but alignment information spreads around more slowly (thus undermining order). At very low densities, when the interaction spheres do not percolate, particle displacement is the only mechanism that can transport orientation information (as opposed to high densities where orientation information is spread by both particle motion and standard diffusion), and thus the last effect turns out to be more important. However, this statement is empirical, based on numerical evidence, and Eq. (1) should be regarded as a phenomenological ansatz. We are not aware of rigorous theoretical arguments regarding the dependence of η_c with v_0.

The aim of this section is thus to study Eq. (1) and estimate the exponents. In particular we want to compute σ, which appears to have received less attention than κ, and to investigate the dependence of both exponents with space dimension (three dimensions have been less studied than two dimensions). We thus set out to compute $\eta_c(v_0, \rho)$ at several speeds and densities. In practice, we measure the average, $\langle \varphi \rangle$, and variance $\mathrm{Var}(\varphi) \equiv \langle \varphi^2 \rangle - \langle \varphi \rangle^2$, of the order parameter as a function η. The critical value of the noise, $\eta_c(v_0, \rho)$ is obtained as the point where $\mathrm{Var}(\varphi)$ is maximum. This is how the critical value of the critical parameter is determined for second-order transitions in finite systems. We remark that although the Vicsek transition has been found to be discontinuous [10,16], this is only evident for rather large system size, while it appears continuous for moderate sizes. For $\rho = 1$ and $v_0 = 0.5$ in two dimensions, about 10 000 particles are required to detect the discontinuous character of the transition, and this number grows rapidly for lower densities and speeds (see Fig. 10 of Ref. [10]). Thus for the sizes we consider, the maximum of the variance of φ is a good measure of the critical noise. If one were to carry out a similar study for much larger sizes, then one should use as an estimate, e.g., the minimum of the Binder cumulant, as in Ref. [10].

Let us consider first the scalar noise case in two dimensions. The order parameter and its variance as a function of noise are shown in Figs. 3 and 4, respectively. Equation (1) suggests defining a rescaled noise as

$$\eta^* = \frac{\eta}{\rho^\kappa}. \qquad (8)$$

Both the average and variance of φ scale reasonably well with η^* (using $\kappa = 1/2$) for all the speeds considered (spanning four orders of magnitude). This implies that $\eta_c \sim \sqrt{\rho}$ in two dimensions in agreement with earlier works [3,8,10,11].
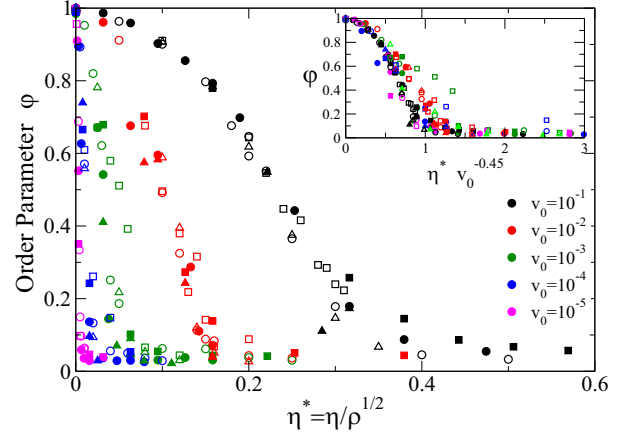

FIG. 3. Two dimensions: Order parameter as a function of the density-rescaled noise ($\eta^* \equiv \eta/\rho^\kappa = \eta/\sqrt{\rho}$) for different N (squares 500, circles $N = 1000$, and triangles $N = 2000$), system densities ρ (full symbols corresponds to density $\rho = 0.1$ and open symbols to $\rho = 1.0$), and velocities v_0 as indicated. Inset: The same data rescaled with a speed-and-density-rescaled noise $= \eta^* v_0^{-0.45}$.

Considering now the rescaled *critical* noise η_c^* as a function of v_0, we also find a power law $\sim v_0^\sigma$ (Fig. 5), with a least-squares fit yielding $\sigma = 0.45(2)$. The value of the exponent showed no significant variation in the range of N studied (from $N = 500$ to $10\,240$). Moreover, it seems that the full order-parameter curves can be scaled using $\eta \rho^{-\kappa} v_0^{-\sigma}$ (inset of Fig. 3). Thus our two-dimensional data are compatible with Eq. (1), with $\kappa = 1/2$, $\sigma = 0.45$. This is in agreement with Ref. [10] for the κ exponent, but not for σ, which these authors found close to 1. However, the speeds used in that article ranged from 0.05 to 0.5, while we have studied considerably smaller speeds, down to $v_0 = 10^{-5}$.
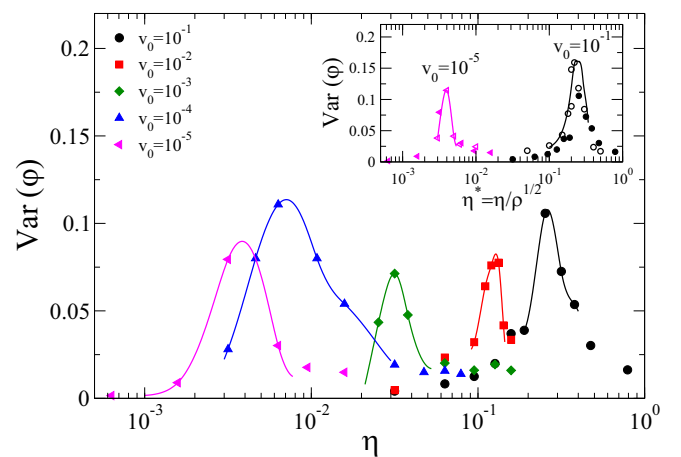

FIG. 4. Two dimensions: Log-linear plot of the fluctuations of the order parameter $\mathrm{Var}(\varphi)$ as a function of noise η for $N = 1000$, $\rho = 0.1$, and speed v_0 as indicated. Inset: The data collapsed with a density-rescaled noise $\eta^* = \eta/\sqrt{\rho}$, for two different speeds $v_0 = 10^{-5}$ and $v_0 = 10^{-1}$, and densities $\rho = 0.1$ (full symbols) and $\rho = 1.0$ (open symbols). In both plots, full lines are guide-to-the-eye splines.
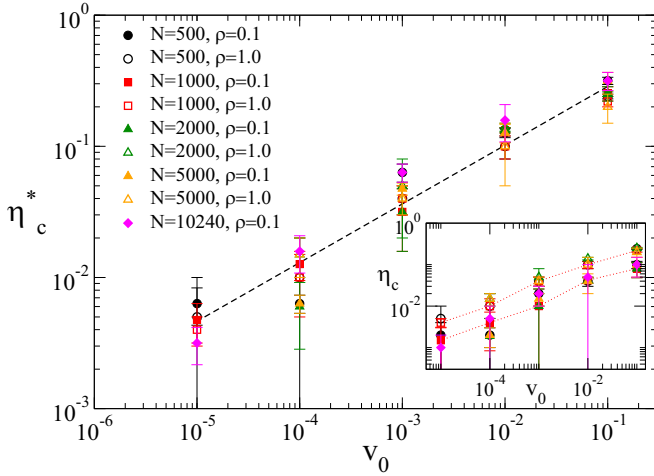
FIG. 5. Two dimensions: Density-rescaled critical noise η_c^* vs speed v_0 for different densities and N, as indicated. Inset: Data before rescaling. Error bars are an upper bound for the error taken from the two points nearest to the maximum computed value of Var(φ).

Turning now to three dimensions, we show the variance of the order parameter versus noise in Fig. 6 (scalar noise). The rescaled noise η^* does not work very well as a scaling variable for the φ or Var(φ) versus noise curves in this case (see the inset of Fig. 6). However, the *critical* noise does scale with ρ^κ, but with $\kappa = 1$ instead of the 2D value $1/2$. This is seen from Fig. 7, where the η_c versus v_0 curves (inset) collapse when using $\eta_c^* = \eta_c/\rho^\kappa$ (main plot). The exponent σ is then obtained fitting η_c versus v_0; we get $\sigma \approx 1/2$, i.e., very close to the 2D case.

In summary, we find that σ is the same in two and three dimensions ($\sigma \approx 1/2$), while $\kappa \approx 1$ in three dimensions and $\kappa \approx 1/2$ in two dimensions. The values of the exponents are rather different from those previously reported for the VM. However, most previous studies used the vector variant of the
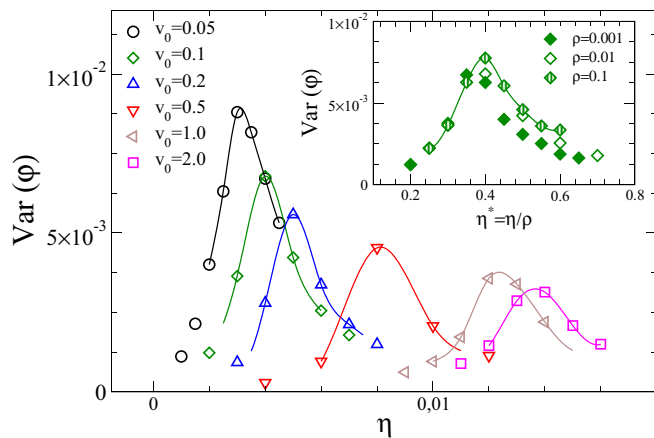

FIG. 6. Three dimensions with scalar noise: Fluctuations of the order parameter Var(ϕ) as a function of noise η, for $N = 1000$, $\rho = 0.01$, and different v_0, as indicated. The value of η that maximizes Var(ϕ) was taken as the critical noise η_C. Inset: Collapse attempt of Var(ϕ) with rescaled noise $\eta* = \eta/\rho$ for $N = 1000$, $v_0 = 0.1$, and three different densities. In both plots full lines are guide-to-the-eye splines.
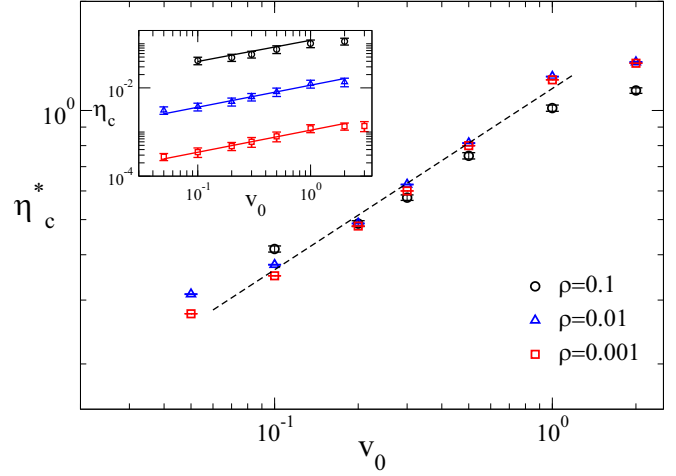

FIG. 7. Three dimensions with scalar noise: Density-rescaled critical noise η_c^* vs v_0 for $N = 1000$ and different densities ρ. Dashed line has slope $1/2$ suggesting that $\eta_C \simeq \sqrt{v_0}$ in the 3D case. Inset: Data before rescaling with density; lines have slope $1/2$. Error bars are an upper bound for the error taken from the two points nearest to the maximum computed value of Var(φ).

VM, so we have also considered vector noise to investigate the effect of the noise rule on these exponents. We computed η_c for different values of speed and density using the Czirók noise rule (5). Since in the vector noise case the first-order character of the transition is evident even at rather small sizes [10], in order to determine η_c, we have used the minimum of the Binder cumulant $U_L \equiv 1 - \frac{\langle\varphi^4\rangle}{3\langle\varphi^2\rangle^2}$. Nevertheless, we have checked that for the sizes we consider, the maximum of the variance of ϕ gives very similar values for η_c. We show η_c versus v_0 and η_c versus ρ for the 3D Vicsek model with vector noise in Fig. 8. The figure also includes points taken from Refs. [10] and [13]. Our results reproduce the previously reported values: the inset of Fig. 8, which shows $\eta_c \sim \rho^{1/3}$ for $v_0 = 0.5$ in agreement with Ref. [10]. However, when going to lower values of v_0, we find strikingly that the slope of the logarithmic plots of the η_c versus ρ curves depends on speed, i.e., that the exponent κ is a function $\kappa(v_0)$: for $v_0 = 0.01$ we find $\eta_c \sim \rho^\kappa$ with $\kappa = 0.63(4)$. Similarly, the η_c versus v_0 slopes depend on density, i.e., $\sigma = \sigma(\rho)$. But this contradicts the ansatz (1): not only is this incompatible with a product of power laws, it implies that η_c cannot be expressed as a product of separate functions of ρ and v_0. So, at least down to $v_0 = 0.01$, the dependence of η_c with noise and density in the 3D VM with vector noise *is not separable,* i.e., it cannot be written as product of a function of ρ times a function of v_0. For $\rho = 0.01$ and 0.1, and speed values $v_0 = 0.1$ and $v_0 = 0.01$, we have also performed simulations of the 3D model with the Grégoire and Chaté rule [Eq. (6)]. The values of η_c obtained from the analysis of the Binder cumulant coincide, within error bars, with the obtained with Eq. (5), at least for the ρ and v_0 values studied. In order to not saturate, these are not been included in Fig. 8.

B. Stationary state and correlation time

We now turn to investigate the dynamic effects of changes in density and speed. Our stationary-state checks allow us to
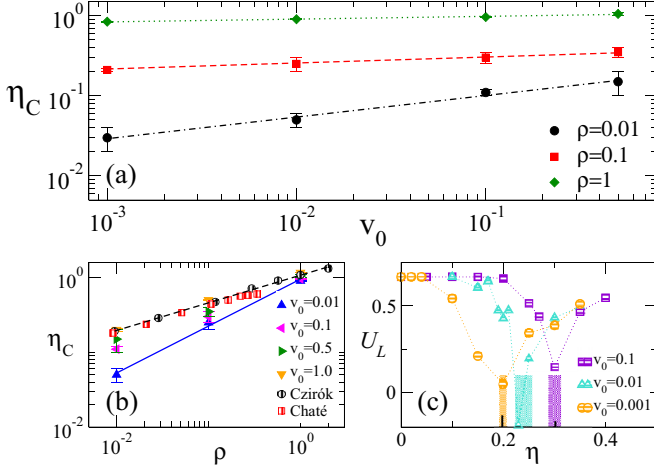
FIG. 8. Three dimensions: (a) Three dimensions with vector noise: η_c vs v_0 for $N = 1000$ and different densities ρ, as indicated. It is seen that η_c depends on ρ as a power law, but the exponent is clearly a nontrivial function of ρ. (b) η_c vs ρ for $N = 1000$, and different v_0, as indicated. The plot includes points taken from the works of Czirók *et al.* [13] and Chaté *et al.* [10]. The slope of the dashed line is $1/3$, the full line has slope 0.63. Error bars are an upper bound for the error taken from the two points nearest to the minimum of the Binder cumulant. (c) Binder cumulant U_L vs η for $N = 1000$, $\rho = 0.01$, and different v_0, as indicated. The value of η_c determined from the minimum of the cumulant is (for the sizes considered) very near the value of the maximum of the susceptibility (shaded region).

investigate these effects by considering the v_0 dependence of t_{st} and τ, i.e., the time to reach a stationary state and the correlation time of the order parameter, respectively (see Sec. II). Figure 2(a) shows how t_{st} was determined from the convergence of the value of the order parameter in two systems starting from complete order and low density, and complete disorder and high density (see Sec. II). Figure 2(b) shows a few instances of the time correlation function of the order parameter (7), from which τ is obtained by an exponential fit. The case shown there corresponds to the critical value of the noise.

If one plots τ or t_{st} versus v_0 at fixed noise and density, one obtains plots such as shown in Fig. 9(a). For large v_0 one seems to get $\tau \sim v_0^{-1}$, but the overall behavior is rather complex and nonmonotonic. The reason is that, since η_c depends on both speed and density, by varying v_0 one can approach (and even cross, as in the example shown) the critical noise. The behavior is simpler if one changes η together with v_0 in a way such that $\eta = X\eta_c(\rho, v_0)$, i.e., keeping at a fixed distance from the critical point. As an example, in Fig. 9(b) we study (for the 2D case) the dependence of τ with speed but fixing the noise such that $\eta = 0.5\eta_c$ (ordered phase), $\eta = \eta_c$, and $\eta = 2\eta_c$ (disordered phase). We find that in the ordered phase the behavior is the same as in the critical region (again varying v_0 and η together to remain at half the critical value). In both cases, the dependence of τ with speed is well described by a power-law behavior as $\tau \propto v_0^\zeta$, with $\zeta \approx -0.75$. On the other hand, in the disordered phase ($\eta = 2\eta_c$), the behavior is more complex and cannot be described by a single power law. If one were to define an effective exponent as the logarithmic
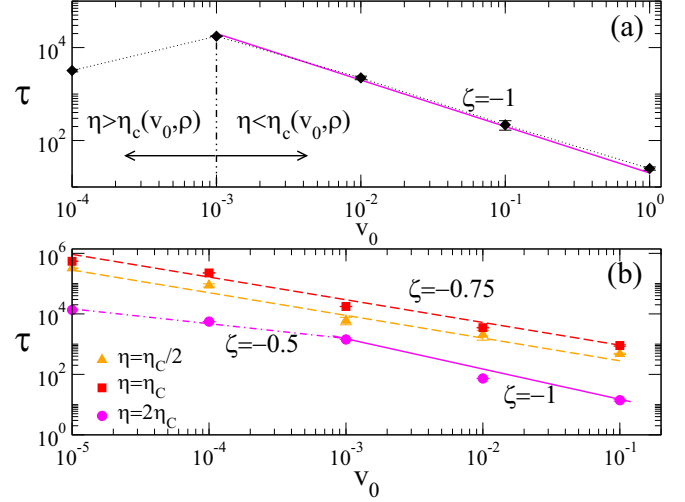

FIG. 9. Two dimensions: (a) τ vs v_0 for $N = 10^3$ and fixed $\eta = 0.01$ and $\rho = 0.1$. The noise corresponds to $\eta_c(v_0 = 10^{-3}, \rho = 0.1)$. (b) τ vs v_0 for $N = 10^3$, $\rho = 0.1$ and different values of η including the ordered and disordered phases. Note that $\eta_c(v_0, \rho)$, so that ρ is varied alongside v_0

derivative of the τ versus v_0 curve, this would seem to go from -1 to -0.5, lowering the speed.

Finally Fig. 10 explores the dynamical effect of varying the speed with the noise fixed at the critical value for both two and three dimensions. Figure 10(a) shows the speed dependence of t_{st} and τ in the 2D scalar noise VM, while Fig. 10(b) shows the same quantities for the 3D case (with scalar and vector noise). We find a similar power-law behavior
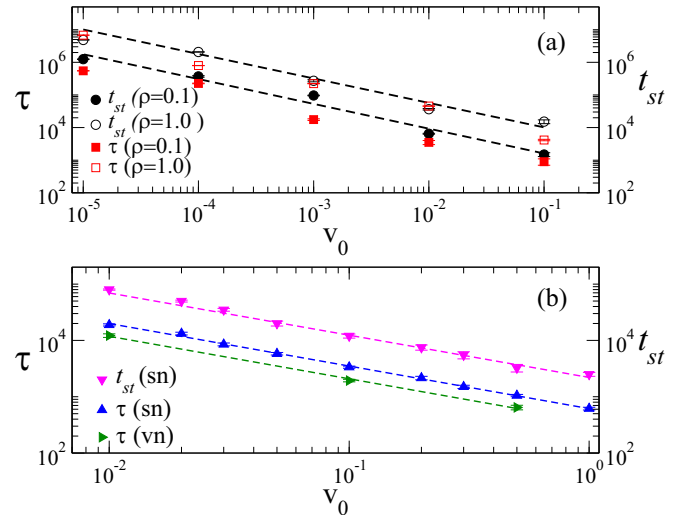

FIG. 10. t_{st} and τ vs v_0 for $N = 10^3$ and $\eta = \eta_c(v_0, \rho)$. (a) 2D case with $\rho = 0.1$ (open symbols) and $\rho = 1.0$ (full symbols). (b) 3D scalar noise (sn) and vector noise (vn), with $\rho = 0.01$. In all cases the dashed line has slope -0.75. Error bars for τ are taken as twice the standard deviation estimated by the least-squares fit. For t_{st}, the error is estimated as the time interval between the first and second crossing of the curves corresponding to the disordered and ordered initial condition (Fig. 2). Note that ρ is varied with v_0 so as to remain at the critical noise.

on both quantities: τ and $t_{\text{st}} \propto v_0^{\zeta}$, and again the points are compatible with $\tau \sim v_0^{-0.75}$.

IV. CONCLUSIONS

We have studied the Vicsek model with scalar noise in two and three dimensions, and the VM with vector noise in three dimensions, at low densities and at lower speeds than in previous studies. Our results support, for the *scalar* noise case in the diluted, low-speed regime, the relation

$$\eta_c \sim v_0^{\sigma} \rho^{\kappa}.$$

We find $\sigma \approx 1/2$ in both two and three dimensions. For the other exponent we find $\kappa \approx 1/2$ in two dimensions, as previously reported, and $\kappa \approx 1$ in three dimensions. Our 3D scalar noise data are not comparable with previous studies, which used the vector noise variant. In two dimensions our κ exponent agrees with previous numerical and theoretical work, but σ is rather lower than the previously reported value (close to 1), in Ref. [10]. A possible source of the disagreement is the much lower values of speed we probed. Since clearly Eq. (1) cannot be valid for all values of density and speed (because η_c is bounded), one expects it to be valid when η_c is small, i.e., in the limit of vanishing speed and/or density. Away from this asymptotic regime, corrections to this scaling law should be expected, and it may well be that if one ignores these corrections one can get a good fit, but with effective exponents different from the asymptotic ones.

Since most previous studies in three dimensions have used the vector noise variant, we have considered also the vector noise VM. We have been able to reproduce earlier results; however, when exploring a wider range of speeds it becomes apparent that while at fixed density the curves look like a power law in speed (and vice versa), the exponent depends on density, a signal that Eq. (1) is not valid in this case, and that the dependence on speed and density is not separable. These results show that the behavior of the diluted VM at low speeds is more complex that hitherto assumed. This is a rather surprising result, pointing to a fundamental qualitative, rather than merely quantitative, effect of the noise rule. This finding implies that the choice of noise has a thermodynamic effect, in the sense that the shape of the $\eta_c(\rho, v_0)$ curve changes qualitatively when changing the noise rule.

In addition to the thermodynamic effect of speed, we have also investigated its effect on the dynamics, specifically the speed dependence of the relaxation time and the time to reach a stationary state independent of initial conditions. When fixing the noise to be a factor of the critical noise, we find in the critical and ordered phases a power law for both quantities, with an exponent that does not depend on space dimension ($\tau \sim v_0^{\zeta}$ with $\zeta = -0.75$). Thus the dynamics are slower for lower speeds, as one would expect given that information flow in $d < 4$ is dominated by convective transport [6]. However, for fixed correlation length, one would guess naively $\tau v_0 = $ const (i.e., $\zeta = -1$), which is inconsistent with our findings except perhaps at relatively large speeds away from the critical point. Another interesting feature is that (at the critical point), ζ is independent of dimension. This suggests that information

propagates anisotropically and is dominated by propagation along one dimension. Such an anisotropy is not too surprising given the known anisotropies in the velocity correlation functions [6]. In any case, the relaxation time for $v_0 = 0$ cannot be divergent (at finite size), so either the relationship breaks down at very low speeds, or the limit $v_0 \to 0$ is singular.

These results underline once more the complexities of the VM due to the coupling between density and order parameter, and call for a more detailed study at very low densities and speeds (particularly for the vector noise case), including (computationally expensive) consideration of finite-size effects.

APPENDIX: ON PERSISTENCE LENGTH

If two particles collide (i.e., their relative distance becomes less than the interaction radius r_c) at low noise, they acquire a common direction with a minor deviation. The persistence length is the distance traveled by either of them before this common direction of motion is washed away by noise. This length can be decomposed in two parts: the distance traveled while interacting (interaction persistence) and the distance traveled as free particles (free persistence).

The free persistence is the easier to estimate: if the particle is free, the direction of the velocity performs a random walk such that $[\Delta\theta(n\Delta t)]^2 \approx \eta^2 n$. Fixing a threshold angle leads to a persistence time $t_{\text{free}} \sim 1/\eta^2$, independent of speed. Since by definition during this time the motion is ballistic we have

$$l_{\text{free}} \sim \frac{v_0}{\eta^2}. \tag{A1}$$

Arguing that at the onset of order this quantity is of the order of the mean-free path $l_p \sim 1/\rho$, one gets $\eta_c \sim \sqrt{v_0 \rho}$. Expression (A1) was derived in Ref. [3] for the persistence length, assuming that the time between collisions is much larger than the time the particles spend interacting. However, this assumption does not hold for very small v_0, as the following estimate for the interaction time shows. At each step the velocities of two otherwise isolated particles will be equal to their average velocity plus noise, so that $[\Delta \mathbf{v}]^2 = 2v_0^2(1 - \cos\theta)$, with θ a random angle in the range $[-2\pi\eta, 2\pi\eta]$. After n steps, the relative square distance is then $[\Delta\mathbf{r}(n\Delta t)]^2 = \sum_{ij}(\Delta t)^2 \Delta\mathbf{v}_i \cdot \Delta\mathbf{v}_j$. Since $\Delta\mathbf{v}_i$ and $\Delta\mathbf{v}_j$ are independent and $\langle[\Delta v]^2\rangle = v_0^2 \langle 1 - \cos\theta \rangle \approx v_0^2 \eta^2$ for small noise, the relative distance performs a random walk, and $\langle[\Delta\mathbf{r}(n\Delta t)]^2\rangle = n(\Delta t)^2 v_0^2 \eta^2$. Equating this to given mutual distance of the order of r_c we obtain

$$t_{\text{int}} \sim \frac{1}{v_0^2 \eta^2}. \tag{A2}$$

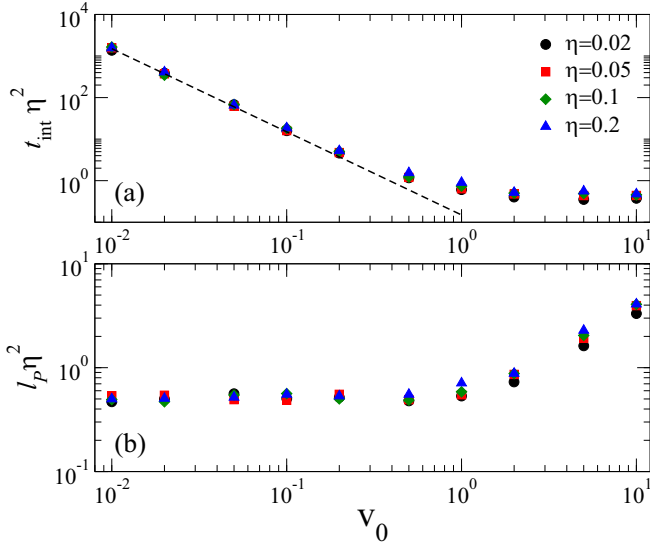Obtaining a length from this time is harder than in the free case, because the motion is not ballistic but is actually a

FIG. 11. (a) Persistence time (t_{int}) times η^2 as a function of speed (v_0), for different η as indicated. Dashed line has slope -2. (b) Persistence length (l_p) times η^2 as a function of speed (v_0). Points were obtained from numerical simulation of two Vicsek particles starting both at the origin and evolving with the stated noise and speed until their velocities lose alignment (the vectors form an angle of $\pi/2$). The results shown are an average over 100 samples.

FIG. 12. Persistence time and length (defined as in Fig. 11) for two particles initially separated by a distance $r_c - v_0$. (a) Persistence time (t_{int}) times η^2 as a function of speed (v_0), for different η as indicated. Line has slope -1. (b) Persistence length (l_p) times η^2 as a function of speed (v_0). Dashed line has slope 1.

(persistent) random walk. For moderate t_{int} (i.e., v_0 not too low) the direction changes little and $l_{int} \approx v_0 t_{int}$, but for low v_0 the time t_{int} gets rather large and the random walk character of the motion starts to become evident. These considerations are confirmed numerically: the (total) persistence time (t_P) [Fig. 11(a)] is proportional to $1/\eta^2$ and goes as $1/v_0^2$ at low speeds. The distance from the origin of the motion (l_P) [Fig. 11(b)], however, does not grow as $1/v_0$. Note, however, that this quantity measures how far the particles are from their initial position when they have lost alignment, while for comparison with the mean-free path a more relevant quantity is the distance traveled along the trajectory, related to the area have swept during the motion (these quantities are different in a random walk).

One may object that in fact a collision means that the two particles come within an interaction radius and it does not
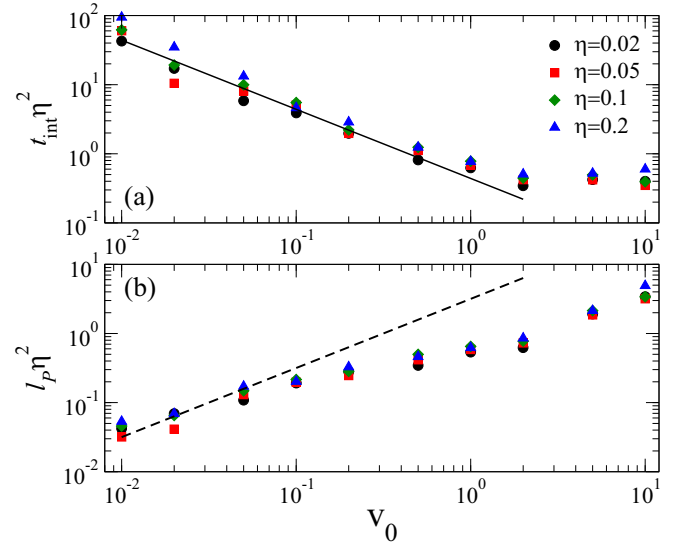
imply that they coincide in space, as the t_{int} estimate assumes. We have repeated the numerical computation exactly as above but with an initial condition where the particles are separated by a distance $r_c - v_0$, which is of the order of the distance between particles that in the previous step were not interacting and now are within each other's interaction circle. The result is shown in Fig. 12(b): $t_{int} \sim 1/(v_0\eta^2)$ and the distance from the initial position $\sim v_0/\eta^2$.

In summary, the collision time at low speeds is long enough to invalidate the argument of Ref. [3]. The last result seems to recover Eq. (A1), but this quantity is the distance from the initial position, and is only a lower bound for the actual distance swept along the trajectory. In any case Eq. (A1) cannot explain the differences that occur when changing dimension or the noise rule. This simple argument, though appealing, is unfortunately not enough to explain the behavior of the VM at low speed.

[1] T. Vicsek, A. Czirók, E. Ben-Jacob, I. Cohen, and O. Shochet, Phys. Rev. Lett. **75**, 1226 (1995).

[2] T. Vicsek and A. Zafeiris, Phys. Rep. **517**, 71 (2012).

[3] F. Ginelli, Eur. Phys. J. Special Topics **225**, 2099 (2016).

[4] D. J. T. Sumpter, Philos. Trans. R. Soc. Lond. B **361**, 5 (2006).

[5] M. C. Marchetti, J. F. Joanny, S. Ramaswamy, T. B. Liverpool, J. Prost, M. Rao, and R. A. Simha, Rev. Mod. Phys. **85**, 1143 (2013).

[6] J. Toner and Y. Tu, Phys. Rev. E **58**, 4828 (1998).

[7] S. Ramaswamy, Annu. Rev. Condens. Matter Phys. **1**, 323 (2010).

[8] A. Czirók, H. E. Stanley, and T. Vicsek, J. Phys. A **30**, 1375 (1997).

[9] A. Czirók, A.-L. Barabási, and T. Vicsek, Phys. Rev. Lett. **82**, 209 (1999).

[10] H. Chaté, F. Ginelli, G. Grégoire, and F. Raynaud, Phys. Rev. E **77**, 046113 (2008).

[11] G. Baglietto and E. V. Albano, Comput. Phys. Commun. **180**, 527 (2009), special issue based on the Conference on Computational Physics 2008.

[12] G. Baglietto and E. V. Albano, Phys. Rev. E **80**, 050103(R) (2009).

[13] A. Czirók, M. Vicsek, and T. Vicsek, Physica A **264**, 299 (1999).

[14] G. Grégoire and H. Chaté, Phys. Rev. Lett. **92**, 025702 (2004).

[15] T. Ihle, Phys. Rev. E **83**, 030901(R) (2011).

[16] A. P. Solon, H. Chaté, and J. Tailleur, Phys. Rev. Lett. **114**, 068101 (2015).